Crystallisation Preferred Orientation in Porous Media

B. Lecampion *Schlumberger Carbon Services, France*

Abstract

The effects of non-hydrostatic stresses on the poro-mechanics of in-pore crystallisation are investigated. The consequences of the hypothesis of a purely hydrostatic state of stress in the crystals on their shape and orientation are derived from a diluted problem following Eshelby's (1957) solution of an inhomogeneous inclusion in an infinite matrix. These results are used in a micro-mechanical scheme to estimate the macroscopic constitutive parameters. The preferred orientation and shape of the crystal, with respect to the stress field, induce a non-linear anisotropic dependence of the macroscopic constitutive parameters of the porous medium upon the stress state. The importance of such an induced anisotropy is explored for a given material as well as the effect of different boundary conditions on a unit volume of material undergoing crystal growth.

1   Introduction

This paper investigates the effect of a non-hydrostatic state of stress on the poro-mechanics of in-pore crystallisation. This type of problem occurs in a wide range of applications in geomechanics, ranging from the observed expansion due to Brucite precipitation in cement (Chatterji, 1995) to the effect of minerals crystallisation associated with CO2 storage (salting-out effect (Fuller et al., 2006), cement carbonation (Kutchko et al., 2007)).

The poro-mechanical effect of confined crystallisation has received an important interest within the scope of in-pore water freezing, and salt-weathering of stones (Ruedrich et al., 2007; Scherer, 1999). A proper picture of the poro-mechanical modelling of such effects has recently arisen (Coussy, 2005; 2006). However, the effect of an anisotropic state of stress on the macroscopic effect of crystallisation has received little attention. Preferred crystallisation orientation has been addressed in the geological literature (Kamb, 1959; Paterson, 1973) with the conclusion that the crystal grows in the direction of the minimum principal stress, but no proper constitutive law, at the level of a representative volume element taking into account such stress modulation effects, seems to have emerged.

This paper follows the work of Coussy (2005; 2006) on poro-mechanics of in-pore crystallisation. However, we address the hypothesis of a hydrostatic state of stress within the formed crystal and its impact on preferred crystallisation orientation in the case of an anisotropic stress field. A dilute configuration of a single crystal embedded in an infinite matrix allows for investigating the consequences of a pure hydrostatic stresses in the crystal on its shape and orientation with respect to the far-field stress. The results of this problem furnish a non-linear relation between the far-field stresses and the geometry of the crystal filled pores. They are further used in a micro-mechanical up-scaling to estimate the unsaturated poro-elastic properties at the level of a representative volume element (Dvorak and Benveniste, 1992). The anisotropy induced on the material properties by non-hydrostatic stresses is investigated for a given material. Finally, examples of restrained and unrestrained boundary conditions on a unit element of a porous material subject to a uniform crystallisation pressure are presented.

2   Crystallisation in porous media

The growth of a crystal occurring in the pore space can lead to large crystallisation pressure which deforms and stresses the porous medium. We quickly review here the main physical phenomena linked to crystal growth in pores (see Scherer, 1999, for more details). The macroscopic constitutive law for such an unsaturated poro-elastic material is then recalled (Coussy, 2007).

2.1 Chemical equilibrium of a single crystal

The condition of chemical equilibrium between the crystal and the pore solution is written in terms of the equality of the crystal and solution chemical potentials. We can write the chemical potential of the solution in the following form (see Dewers and Ortoleva, 1988; Scherer, 1999):

$$\mu_l = \mu_l^*(p_l, T) + RT \log a \tag{1}$$

where a denotes the activity of the solution, μ_l^* is a reference chemical potential (function of temperature) and R is Boltzman constant. The crystal chemical potential is expressed as:

$$\mu_c = \mu_c^*(T) + \rho_c^{-1}(p - p_o) \tag{2}$$

where ρ_c is the crystal molar density and p is the normal stress applied to the crystal. The contribution of the elastic molar strain energy on the crystal chemical potential has been neglected due to the small effect for stresses under 100 MPa (see Durney, 1976; Paterson, 1973) and others for discussion).

Chemical equilibrium implies that $\mu_l = \mu_c$ at all points along the crystal-solution interface. When a crystal is not uniformly loaded, the faces under larger confining stresses have thus a higher solubility. In the case where a crystal grows in pore, a thin film of fluid is typically present between the crystal and the pore walls. Such a film of fluid allows the diffusion of ions around the crystal such that ultimately the activity of the solution around the crystal reaches an equilibrium value a, and so does the pressure p_c in the crystal. The equality of the chemical potential furnishes the so-called Correns equation:

$$p_c - p_l = \frac{RT}{\rho_c^{-1}} \log\left(\frac{a}{a_o}\right) \tag{3}$$

where a_o is the activity of the solution corresponding to the equilibrium of the solution with a large crystal at the solution pressure p_l and temperature T. In what follow, we will assume that the diffusion in the thin-film of fluid between the crystal and the matrix is "fast" such that only the equilibrium state described by Equation (3) is taken into consideration (hypothesis of fast grain-boundary diffusion).

As well as Equation (3), one has to recall that the continuity of normal stresses between the crystal and the solution is ensured by the capillary pressure linked to the interface energy γ_{cl}:

$$p_c - p_l = \gamma_{cl} \kappa_{cl} \tag{4}$$

where κ_{cl} denotes the curvature of the crystal / liquid interface. The effect of a number of pore geometry has been investigated in the literature (Coussy, 2006; Flatt, 2002; Scherer, 1999). In the simple case of a crystal growing from a large spherical pore into a smaller one, the capillary pressure is governed, at first order, by the pore entry radius of the smaller pore: $p_c - p_l = 2\gamma_{cl} / r_e$. The preceding equation (known as the Laplace equation) relates the pressure difference between a wetting and a non-wetting fluid to the interface energy and the surface curvature. It describes capillarity effect at the level of one pore throat. The up-scaling of such an equation (valid at the level of one pore) to a complex porous network is non-trivial but can be adequately grasped via the pore-size distribution of the porous media within a representative volume element (RVE) of the porous material (Coussy, 2006). For a given value of the capillary pressure $p_c - p_l$ corresponds a given

pore entry radius r_e via Laplace's equation: $r_e = \dfrac{2\gamma_{cl}}{p_c - p_l}$. Moreover, it has been observed that the crystal tends to grow first in larger pores where the solubility of the crystal is lower thanks to a lower capillary pressure (Rijniers et al., 2005).

This allows to relate the crystal saturation S_c in the Representative Volume Element to the cumulative pore-size distribution D of the material and the pore entry radius r_e:

$$S_c = 1 - D(r_e) = 1 - D\left(\frac{2\gamma_{cl}}{p_c - p_l}\right)$$
(5)

Such a link between the crystal saturation and the capillary pressure provides a way of connecting the porous network at the level of the representative volume element, as discussed by Coussy (2006).

2.2   Poro-mechanics for crystallisation in pores

Coussy has developed a consistent framework for un-saturated porous media that has been applied to crystallisation (Coussy, 2005; 2006; 2007). The porosity ϕ is split in two parts at the level of the representative element: crystal ϕ_c and liquid filled pores φ_l ($\phi = \phi_c + \phi_l$). The crystal (S_c) and liquid saturation ($S_l = 1 - S_c$) are defined with respect to the initial porous volume prior to any deformation, and have thus been coined as Lagrangian saturation. The variation of the crystal porosity φ_c comes either from an increase of the crystal saturation or the mechanical deformation of the current crystal porosity. It is therefore decomposed as:

$$\phi_c = \phi_o S_c + \varphi_c$$
(6)

where ϕ_o is the initial porosity of the porous medium prior to any deformation and φ_c is the variation of the crystal porosity associated with the skeleton deformation. A similar decomposition holds for the fluid-filled part of the porosity ϕ_l.

Under the assumption of linear isotropic elasticity, the following constitutive law can be derived from thermodynamic principles (see Coussy, 2006) for a complete derivation):

$$\sigma_{ij} = 2G\varepsilon_{ij} + (K - 2/3G)\varepsilon^v \delta_{ij} - b_c p_c \delta_{ij} - b_l p_l \delta_{ij}$$
(7)

$$\varphi_l = b_l \varepsilon^v + \frac{p_l}{N_{ll}} + \frac{p_c}{N_{cl}}$$
(8)

$$\varphi_c = b_c \varepsilon^v + \frac{p_l}{N_{lc}} + \frac{p_c}{N_{cc}}$$
(9)

where b_J, N_J are the generalised Biot coefficients and coupling moduli respectively. These coefficients are function of the crystal saturation. $\sigma_{ij}, \varepsilon_{ij}$ and ε^v have their usual meaning: stress, strain tensors and volumetric strain. It is important to note that Equation (5) linking the capillary pressure $p_c - p_l$ to the crystal saturation via the cumulative pore-size distribution closes the constitutive relations describing the behaviour of the porous media.

In the derivation of the preceding constitutive law, the crystals in the pore space were treated as "voids" with an internal pressure equal to the crystal pressure p_c. The elastic properties of the crystal therefore do not enter in this macroscopic constitutive law of the porous media. Such a model rests on the assumption that no shear stresses develop within the crystal: the crystal is under a uniform hydrostatic pressure p_c. This assumption is consistent with the chemical equilibrium configuration where the activity of the solution surrounding the crystal is uniform (see previous section). However, this hypothesis of a hydrostatic state of stresses within the crystal requires a more detailed analysis especially with regard to the equilibrium shape of the crystal in the case of an anisotropic stress field. One has to recall that the chemical equilibrium, described by Equation (3), supposes that the activity is uniform in the pore solution around the crystal.

In the case where the crystal is non-hydrostatically stressed, it will have to change its shape in order to reach the same value of solubility everywhere (see Durney, 1976; Scherer, 1999, for discussion). The hypothesis of a hydrostatic stress state in the crystal is investigated from a mechanical point of view in the following section.
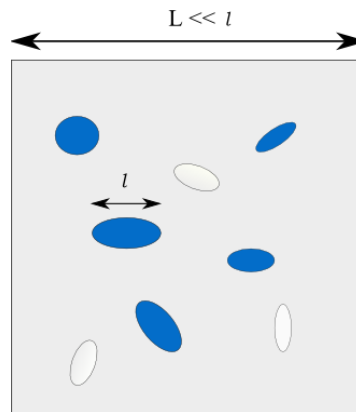

Figure 1   A representative volume element of a porous medium containing fluid (dark) and crystal filled (white) pores

3   Hydrostatic stress postulate

In this section, we investigate the postulate stating that the stresses within a crystal growing in a porous media remain hydrostatic thanks to a film of fluid between the crystal and the pore wall. In order to understand the causes and consequences of such a strong statement, we focus on a single crystal filling a pore of the material. Moreover, we simply model the crystal as an ellipsoid inclusion embedded in an infinite matrix. The crystal and the matrix are assumed to follow an isotropic elastic behaviour. Such a simple model, often refer to as a dilute problem, allows to grasp the first order physical phenomena at stakes while providing the basis for any up-scaling scheme that will further include the interaction between the different inclusions inside a representative volume element.

Let's first recall a number of results. The case where the ellipsoid inclusion remains fully bonded to the matrix corresponds to the classical Eshelby's (1957) solution. The bonding condition implies continuity of the stresses and displacement at the crystal-matrix interface: typically shear forces will be present along the interface. For a given crystal geometry, the shear stresses inside the crystal will vanish for any far-field stress only if the crystal possesses a vanishingly small shear modulus. This is however rarely the case, such that for a typical crystal, other conditions are required in order to satisfy a hydrostatic state of stress inside the crystal inclusion.

Let's now consider the presence of a thin-film of water which "decouples" the crystal from the matrix. One has therefore to investigate the case of a pure sliding condition between the matrix and the crystal. Such a boundary condition consists in the continuity of the normal stress and normal displacement across the crystal-matrix interface while shear forces vanish along this interface. A number of solutions for such problems actually exists (Huang and Mura, 1992; Mura and Furuhashi, 1984; Mura et al., 1987). These solutions are obtained by superposing Eshelby's (1957) solution and the stress field due to a Volterra dislocation of proper intensity along the inclusion / matrix interface (see Huang et al., 1993, for details). Two important conclusions result from these solutions:

- For a spherical crystal, non-hydrostatic far-field stresses will still result in shear stresses within the inclusion despite a pure sliding condition at the crystal-matrix interface (Mura and Furuhashi, 1984).

- For a non-degenerate ellipsoid crystal, in the case of a far-field stress of pure shear nature ($\sigma_{ii} = 0, i = 1, 3$) with respect to the ellipsoid axis, the stresses vanish in the crystal which can therefore be treated as a void (Furuashi et al., 1992; Mura et al., 1987).

In light of these results, we see that a purely sliding condition alone is not sufficient to ensure that the stresses in the crystal inclusion remain hydrostatic for any given far-field stresses. In order for the stresses within the crystal to be hydrostatic, the growing crystal has to adapt itself to the far-field stress, i.e. change its shape accordingly.

In the coordinates system defined by the direction of the far-field principal stresses, we will look for the dimensions of the ellipsoid crystal that minimise the deviatoric stresses within the crystal. In the absence of a complete analytical solution for a purely sliding ellipsoid inclusion, we will use Eshelby's solution (bonded case). The small amount of shear stress in the crystal with such an optimal shape will ultimately justify the use of the bonded solution. Larger shear stresses will not occur if sliding is allowed between the inclusion and the matrix. Having such an optimal shape of the crystal in hands (for a given far-field stress), we will be able to perform an up-scaling of the poro-mechanical properties of the medium assuming hydrostatic stresses within the crystal filled pores of ellipsoidal shape.
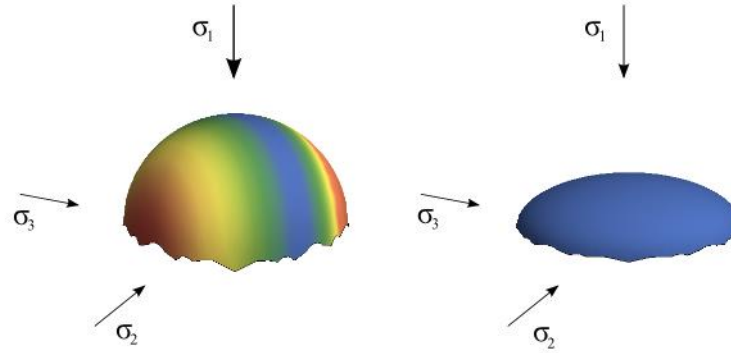

Figure 2 **Contour of shear forces on the surface of the crystal inclusion for a given far-field stress state $\sigma_1 = 1.4, \sigma_2 = 1.1, \sigma_3 = 1$. In the case of a spherical crystal (left) and an ellipsoid crystal (right) with optimum aspect ratios $(\alpha = 0.752, \beta = 0.42)$, the shear force disappears in the case of the optimum ellipsoid (right)**

3.1 Optimal crystal shape

We define the optimal crystal shape as the shape of the ellipsoid crystal for which the deviatoric stresses within it are the lowest for a given far-field stress, matrix and crystal elastic properties. We minimise the value of the second invariant of the deviatoric stress tensor J_2 in the crystal as a function of the ellipsoid dimensions, using Eshelby's solution for an inhomogeneous ellipsoid in an infinite matrix. We suppose that the axis of the ellipsoid coincides with the direction of the principal far-field stresses $(\sigma_1, \sigma_2, \sigma_3)$ taken positive in compression (Figure 2). It is possible to let the axis of the ellipsoid be in a different orientation than the principal stresses, but the optimum shape is actually always aligned with the principal stress direction. We scale the semi-axis dimensions (a_1, a_2, a_3) of the ellipsoid by the dimension in direction of the minimum stresses a_3. The deviatoric stress invariant J_2 is thus a function of the two remaining dimensionless aspect ratio $\alpha = a_2 / a_3$ and $\beta = a_1 / a_3$. For a given far-field stress, we minimise J_2 in function of α and β via a Nelder–Mead Simplex algorithm. We can anticipate easily that the two optimum aspect ratios of the ellipsoid, for which the stress invariant J_2 in the crystal is minimum, are actually solely the function of the corresponding principal stresses ratios σ_2 / σ_3 and σ_1 / σ_3. It is however easier for clarity to keep the usual description of the stress tensor in terms of principal stresses, deviatoric and mean stresses. Moreover, in all cases, the far-field stress tensor can always be scaled by a characteristic value. All the examples presented in this section have therefore stresses of order one.

In the following examples, the bulk and shear moduli of the matrix is taken to $k_m = 5.5$ GPa and $g_m = 4.1$ GPa, while the bulk and shear moduli of the crystal inclusion are taken to be twice larger than the matrix value, otherwise stated.

As a first illustration, we investigate the evolution of the aspect ratio when the far-field stress departs from a hydrostatic state where the sphere ($\alpha = \beta = 1$) is *always* the optimal shape. Figure 3 displays the evolution of the aspect ratio β with the increase of the principal stress σ_1 for a constant value of the other two principal stresses $\sigma_2 = \sigma_3 = 1$ (α remains equal to unity as a consequence). The ellipsoid gets smaller in the direction of the maximum compressive stress: the crystal tends to orient itself in the direction of the minimum stress. One has also to note that the mismatch of the elastic moduli between the matrix and the crystal is a critical parameter in the evolution of the ellipsoidal shape. A stiffer crystal tends to "delay" the deviation from the spheroid shape (Figure 3).
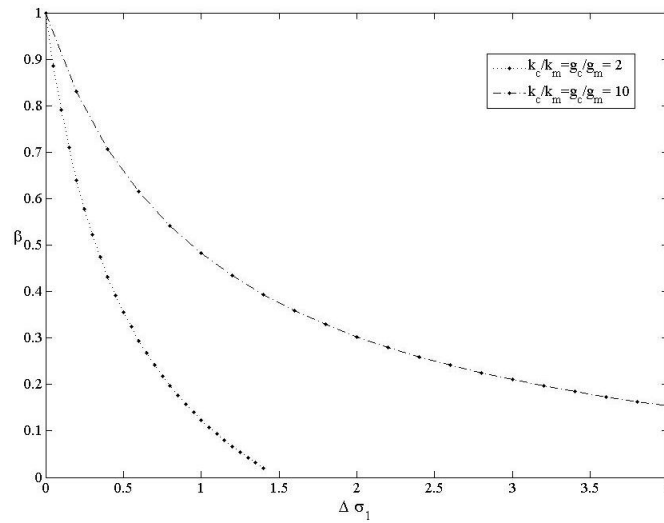

Figure 3 **Evolution of the ellipsoid aspect ratio when the maximum stress σ_1 is increased (keeping $\sigma_2 = \sigma_3 = 1$) for two different ratio of the matrix and crystal elastic moduli ($k_m / k_c = g_m / g_c$)**

Another illustrative evolution of the stress state corresponds to the case where the deviatoric components of the stress tensor (i.e. $\sigma_1 - \sigma_3$ and $\sigma_2 - \sigma_3$) remain constant while the mean stress $(\sigma_m = \frac{1}{3}(\sigma_1 + \sigma_2 + \sigma_3))$ increases. Figure 4 displays such an evolution for $\sigma_1 - \sigma_3 = 1.2$ and $\sigma_2 - \sigma_3 = 0$. It is interesting to note that for a higher value of the mean stresses, a smaller deviation from the spheroid shape is observed.

For all the cases encountered, the minimum value of J_2 obtained for the optimal shape is on the order of 10^{-8}. A crystal inclusion with an optimal shape with respect to the far-field stress is therefore under a purely hydrostatic state of stress. In the case of crystal growth from solution, such an optimum shape of the crystal is completely consistent with the chemical equilibrium described by Correns Equation (3). The uniform value of the pore solution's activity around the crystal is ensured by the hydrostatic pressure within the crystal having its optimal shape with respect to the far-field stresses.
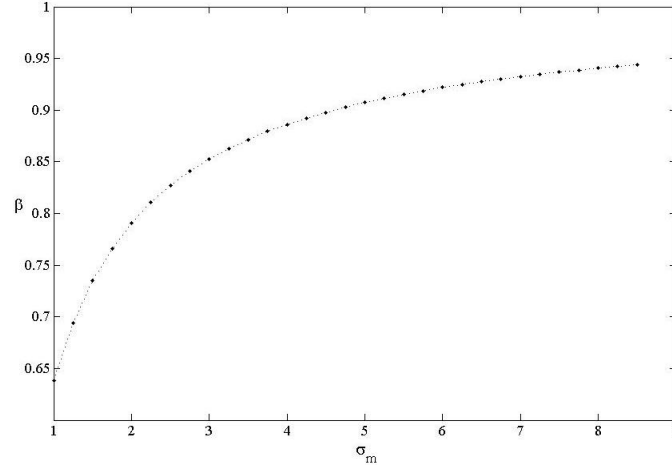
Figure 4   **Evolution of the ellipsoid aspect ratio when the mean stresses increase while keeping the deviatoric components constant:** $\sigma_1 - \sigma_2 = 1.2$, $\sigma_2 - \sigma_3 = 0$

4   Macroscopic constitutive law

The results of the preceding section have highlighted the effect of an anisotropic stress state on crystal shape and orientation. It is possible to use the non-linear relation between the crystal aspect ratio α, β and the stress state to enhance the macroscopic constitutive law Equations (7) to (9). The elastic moduli, Biot coefficients are now stress dependent and anisotropic (as soon as the stresses are). We can re-write the constitutive laws Equations (7) to (9) as follow:

$$\boldsymbol{\sigma} = \mathbf{L}\boldsymbol{\varepsilon} - \mathbf{b}_l p_l - \mathbf{b}_c p_c$$

$$\Delta\varphi_l = \mathbf{b}_l \boldsymbol{\varepsilon} + \frac{p_l}{N_{ll}} + \frac{p_c}{N_{lc}}$$

$$\Delta\varphi_c = \mathbf{b}_l \boldsymbol{\varepsilon} + \frac{p_l}{N_{cl}} + \frac{p_c}{N_{cc}}$$

(10)

where all the material parameters are now function of the stress state: $b_c = b_c(\sigma)$, etc. The non-linear dependence of the material parameters with the stress state can be obtained from a up-scaling scheme of the dilute problem described in the previous section. This is performed using the results of Dvorak and Benveniste (1992). See also Berryman (1997), Nemat-Nasser and Hori (1999), Zaoui (2002) for an introduction to micro-mechanics. We briefly recall here the hypothesis and results of such a micro-mechanical up-scaling.

4.1   Micro-mechanical estimates

We consider a RVE of a porous media of porosity ϕ having fluid and crystal filled pores with respective saturations S_c and $S_l = 1 - S_c$. The representative volume element is defined by the length-scale L which must be much greater than the length-scales 1_i of the different constituents of the material at the micro-scale in order to statistically represent the local continuum properties of the medium. We restrict ourselves to the case where the crystal and fluid filled pores have two distinct length scales sufficiently different from one another. In particular, we assume that the crystal filled pores are larger than the fluid filled pore so that we can consider the material at the scale of the RVE as a composite made of a porous matrix (containing the fluid filled pores) *and* the crystal filled pores with an internal pressure p_c. This model is consistent with the observation that crystals first grow in the larger pores. Obviously, for large crystal saturation, such a

simplification becomes questionable. We suppose that the fluid saturated porous matrix of porosity $\phi_m = \frac{\phi(1-S_c)}{1-S_c\phi}$ follow a linear isotropic poro-elastic constitutive law:

$$\boldsymbol{\sigma}_m = \mathbf{L}_m \boldsymbol{\varepsilon}_m - b_m p_l \mathbf{I} \tag{11}$$

$$\Delta\varphi_m = b_m \varepsilon_m^v + \frac{p_l}{N_m} \tag{12}$$

where $\mathbf{L}_m$ is the tensor of the matrix drained elastic moduli (isotropic), b_m and N_m are the matrix Biot coefficient and modulus respectively. p_l denotes the fluid pressure inside the fluid-filled pore of the matrix.

The crystal filled pores (under a uniform hydrostatic pressure p_c) are the other constituents of the material. The volume fraction of the crystal filled pore is simply equal to $S_c\phi$. One has to remember that the shapes of these pores are obtained (for a given value of the macroscopic stresses) by minimising the shear stresses within a fully bonded crystal inclusion with the elastic properties of the crystal (see previous section). For a given stress state, the crystal filled pores are thus modelled as an ellipsoidal void of optimal shape with the corresponding ellipsoidal shape under a uniform hydrostatic pressure p_c in order to obtain the relevant constitutive parameters at the scale of the RVE. Finally, the total porosity ϕ of the material is equal to:

$$\phi = \phi_m(1-S_c\phi) + S_c\phi = \phi_l + \phi_c \tag{13}$$

One has to recall that the variation of the crystal (or fluid) filled pores porosity comes from a variation of crystal saturation and the deformation of the porous skeleton. Following the definition introduced by Coussy (2006; 2007) of a Lagrangian saturation defined with respect to the non-deformed state, the mechanical deformation of the porosity for a given crystal saturation is split in two parts: the deformation of the crystal filled $\Delta\varphi_c$ and fluid filled pores $\Delta\varphi_l = (1-S_c\phi)\Delta\phi_m$.

4.1.1 Estimate of elastic moduli and Biot coefficients

The approach developed by Dvorak and Benveniste (1992), also known as transformation field analysis, allows us to obtain up-scaled multi-phases elastic media having piece-wise uniform transformation eigenstrain (or eigenstress) in each phase. We follow these results in order to consistently obtain the up-scaled properties of the porous medium of interest. In particular, the macroscopic elastic moduli tensor is simply obtained as:

$$\mathbf{L} = (1-\phi S_c)\mathbf{L}_m \mathbf{A}_m \tag{14}$$

where $\mathbf{A}_m$ denotes the matrix strain concentration tensor. The Biot coefficients linked to the crystal and liquid filled pores are obtained from application of Hill's lemma:

$$\mathbf{b}_l = (1-\phi S_c)\mathbf{A}_m \mathbf{I} b_m \tag{15}$$

$$\mathbf{b}_c = \phi S_c \mathbf{A}_c \mathbf{I} \tag{16}$$

where $\mathbf{A}_c$ is the matrix strain concentration tensor. The average in the RVE of the concentration tensors A_c and $\mathbf{A}_m$ is equal to unity: $(1-\phi S_c)\mathbf{A}_m + \phi S_c \mathbf{A}_c = \mathbf{I}$.

4.1.2 Variation of porosities

The deformation of the liquid and crystal filled pores can be related to the macroscopic strain, fluid and crystal pressures. These constitutive relations are actually intrinsically related to the so-called localisation problem which consist in finding a relation between the macroscopic stress and strain on the RVE (σ, ε) and the 'local' quantities in each phase r (σ_r, ε_r). In the case where transformation eigenstress (i.e. internal pressure) is present in each phase, an additional effect has to be taken into account, compared to the simpler case of purely elastic phases. This problem has been solved consistently by Dvorak and Benveniste (1992) in the case of piece-wise uniform eigenstrain in the different phases. Their results therefore directly apply to porous media where the pressure in the pores is uniform. We will not detail here this approach. It is based on the solution of the so-called transformation eigenstrain concentration tensors. It allows us to recover the volumetric deformation of the crystal and fluid described in the last two equations of the macroscopic law Equation (10) and the expression of the Biot modulus are given by:

$$N_{ll}^{-1} = (1 - \phi S_c)\left(\mathbf{JD}_{mm}\mathbf{M}_m\mathbf{I}b_m^2 + \frac{\mathbf{I}}{N_m} \right) \tag{17}$$

$$N_{lc}^{-1} = (1 - \phi S_c)\mathbf{JD}_{mc}\mathbf{M}_c\mathbf{I}b_m \tag{18}$$

$$N_{cl}^{-1} = \phi S_c\mathbf{JD}_{cm}\mathbf{M}_m\mathbf{I}b_m \tag{19}$$

$$N_{cc}^{-1} = \phi S_c\mathbf{JD}_{cc}\mathbf{M}_c\mathbf{I} \tag{20}$$

where $\mathbf{M}_r = \mathbf{L}_r^{-1}$ is the compliance tensor of phase r, J the fourth rank volumetric tensor ($J_{ijkl} = \frac{1}{3}\delta_{ij}\delta_{kl}$). $\mathbf{D}_{rs}$ is the eigenstrain concentration tensor taking into account the interaction between phases r and s. In the case of a composite material $(n = 2): r = m, c$, the transformation concentration tensors can actually be directly expressed in function of the phases properties (see Dvorak and Benveniste, 1992, for details and extension to multiple constituents):

$$\mathbf{D}_{rm} = (\mathbf{I} - \mathbf{A}_r)(\mathbf{L}_m - \mathbf{L}_c)^{-1}\mathbf{L}_m, \mathbf{D}_{rc} = -(\mathbf{I} - \mathbf{A}_r)(\mathbf{L}_m - \mathbf{L}_c)^{-1}\mathbf{L}_c \tag{21}$$

4.1.3 Macroscopic estimates

The macroscopic estimates of the different constitutive parameters can be obtained from the porous matrix parameters, the crystal shape and saturation using the different Equations (14), (16) and (20). They only depend on the knowledge of the localisation tensor $\mathbf{A}_r$. All the different estimates of the elastic moduli derived in the literature differ only in the way the concentration factors are approximated. The same applies to the estimates of the poro-elastic coupling coefficients. Restricting to random materials (without any periodic structure of the different phases), the first approximation consists of neglecting the interaction between the different inclusions. Under such hypothesis, the solution to the problem of a single ellipsoidal inclusion in an infinite matrix (i.e. Eshelby's solution (1957)) provides the expression of the concentration tensor of the inclusion. Such a dilute estimation of the macroscopic is only valid for small volume fraction of the inclusion such that the interaction between the different inclusions can be neglected. In order to take into account the interaction between inclusions, the effective medium method takes into account an appropriate average matrix stress. The most common estimates are the Mori–Tanaka and self-consistent estimates (Nemat-Nasser and Hori, 1999). In both cases, the concentration tensor can be written as follow:

$$\mathbf{A}_r = \left(\mathbf{L}^* + \mathbf{L}_r\right)^{-1}\left(\mathbf{L}^* + \mathbf{L}\right) \tag{22}$$

where $\mathbf{L}^*$ is the so-called Hill's tensor which is directly related to Eshelby's tensor $\mathbf{S}$ as $\mathbf{L}^*\mathbf{S} = \mathbf{L}(\mathbf{I} - \mathbf{S})$.

In the Mori–Tanaka method, $\mathbf{L}^*$ is evaluated for an inclusion in the matrix of moduli $\mathbf{L} = \mathbf{L}_m$, while in the self-consistent method it is evaluated for an inclusion in the effective homogeneous medium with overall macroscopic moduli $\mathbf{L}$.

4.2   Importance of the induced anisotropy

The properties of the matrix are taken as follow: $k_m = 5.5$ GPa, $g_m = 4.1$ GPa, $b_m = 0.65$ while the total porosity and the crystal saturation are taken respectively as $\phi = 0.2$ and $S_c = 0.3$. The Mori–Tanaka estimates of the different constitutive parameters (drained elastic moduli, crystal filled and fluid filled pore Biot coefficients etc.) are obtained for a given macroscopic stress state from the corresponding optimal shape of the crystal inclusion. The optimal shape is obtained by minimising the deviatoric stresses within the elliptical inclusion having the elastic properties of the crystal: $k_c = 2k_m$, $g_c = 2g_m$ under the given far-field macroscopic stress state.

We are interested, in particular, in the relative variation of the constitutive parameters from their value for spherical crystals (for which the material is isotropic). One can observe that the relative variations of the Biot coefficients (Figures 5 and 6) are more than ten times larger than the maximum relative variation of the drained elastic and Biot moduli (not shown here). This reveals that the induced anisotropy has a first order effect on the crystal Biot coefficients whereas the effect on the macroscopic elastic moduli and the Biot modulus is less pronounced. The large induced anisotropy on the Biot coefficient tensor $\mathbf{b}_c$ is extremely important as it "orients" the macroscopic effect of the crystallisation pressure with respect to the macroscopic stresses, thus providing a non-linear coupling between stress and strain induced by the crystallisation pressure.

In order to remain consistent with the hypothesis that the state of stress within the crystal remains hydrostatic, the shape of the crystal "adapts" to the macroscopic stress present within the representative volume element. In order to grasp the influence of such an optimal shape on the value of the macroscopic parameters, we investigate the example, discussed in the previous section, where the maximum principal stress is increased from a hydrostatic state.
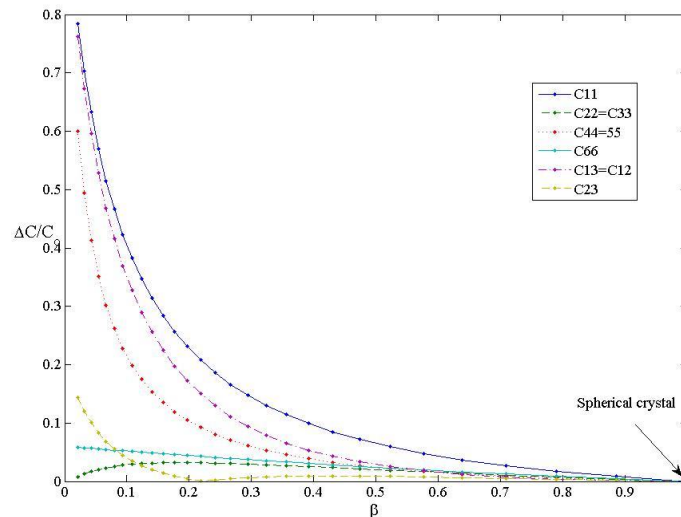

Figure 5   **Relative variation of the elastic coefficients (Voigt notation) from the case of a hydrostatic stress state (spherical crystal) for different value of the crystal aspect ratio β**
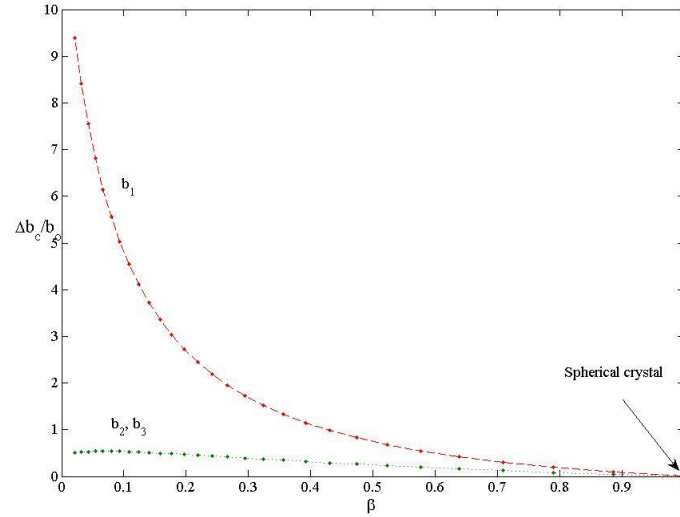
Figure 6 **Relative variation of the crystal Biot coefficients from the case of a hydrostatic stress state (spherical crystal:** $b_c^1 = b_c^2 = b_c^3 = b_c^o$ **) for different value of the crystal aspect ratio** β

5 Investigation of simple boundary conditions

Let's now investigate, for constant crystal saturation and a constant crystallisation pressure, the effect of simple boundary conditions on a representative volume element. In the following examples, we will neglect the variation of the macroscopic elastic moduli due to the crystal shape modulation and focus on the effect induced by the variation of the crystal Biot coefficients. The material therefore remains isotropic except for the values of the Biot coefficients. Moreover, drained conditions for the fluid are also assumed: the fluid diffusion timescale is supposed to be sufficiently small compared to the time-scale associated with crystal growth. We therefore neglect the effect of any fluid pore pressure on the skeleton deformation. The crystallisation pressure is here simply taken as a constant and no link to the chemical equilibrium is investigated.

5.1 Unrestrained configuration

In the case, where a unit volume of the porous medium is un-restrained and free of external stresses, the volumetric deformation induced by the crystallisation pressure results in an isotropic expansion. Due to the hydrostatic state of stress, the optimal shape of the crystal is a sphere which results in an isotropic value of the Biot coefficients $\mathbf{b}_c = b_c^o \mathbf{I}$. The volumetric expansion is simply:

$$\varepsilon^v = \frac{b_c^o p_c}{K} \tag{23}$$

where K is the drained bulk moduli of the porous material.

5.2 1D restrained configuration ($\varepsilon_z = 0$)

As soon as one axis of the unit element is restrained in one direction (i.e. $\varepsilon_z = 0$), the state of stresses induced by the crystallisation pressure is therefore no more hydrostatic. This, in turn, results in a preferred orientation of the crystal and anisotropic values of the crystal Biot coefficients: $b_c = \left(b_x, b_y, b_z \right)$ in the principal stress direction. The faces that are not restrained, are free of stresses: $\sigma_x = \sigma_y = 0$. The strain along the stress free directions and the stress in the restrained direction are simply obtained from the constitutive Equation (10) as:

$$\varepsilon_x = \varepsilon_y = \frac{1}{2}\varepsilon^v = \frac{b_x(\sigma_z)p_c}{2/3(G+3K)} \tag{24}$$

$$\sigma_z = 2(K-2/3G)\varepsilon_x - b_z(\sigma_z)p_c \tag{25}$$

where we have highlighted the non-linear dependence of the Biot coefficients on the state of stress. In this case, two principal stresses are equal ($\sigma_x = \sigma_y$) such that two of the principal Biot coefficients are also equal: $b_x = b_y$. For a given value of stress, the optimal shapes of the crystals are obtained by minimising the deviatoric stress within an ellipsoid inclusion (dilute problem). The Biot coefficients are obtained from a Mori–Tanaka micro-mechanical scheme for the corresponding aspect ratio of the ellipsoidal crystal inclusion. The previous system of Equation (25) is therefore non-linear. We use a simple Picard-type iterative algorithm to solve such a system starting from a trial value for σ_z: $\sigma_z^0 = 0$. At a given iteration k, a new estimate of the only non-vanishing stress σ_z is obtained as follow:

$$\sigma_z^k = 2(K-2/3G)\frac{b_x(\sigma_z^{k-1})p_c}{2/3(G+3K)} - b_z(\sigma_z^{k-1})p_c \tag{26}$$

Convergence is reached for $\|\sigma_z^k - \sigma_z^{k-1}\| < 10^{-5}$ usually in less than ten iterations.

5.3   2D restrained configuration ($\varepsilon_y = \varepsilon_z = 0$)

In the case where two directions of the unit volume are restrained ($\varepsilon_y = \varepsilon_z = 0$) and the other direction is free of stress ($\sigma_x = 0$), the non-vanishing strain and stress components are simply:

$$\varepsilon^v = \varepsilon_x = \frac{b_z(\sigma_z)p_c}{K+4/3G} \tag{27}$$

$$\sigma_y = \sigma_z = (K-2/3G)\varepsilon^v - b_z(\sigma_z)p_c \tag{28}$$

Similarly, as for the 1D restrained case, the crystal Biot coefficients: $b_x, b_y = b_z$ are functions of the stress state ($\sigma_x = 0, \sigma_y = \sigma_z$). This non-linear system is solved with a similar Picard type iterative algorithm other than for the 1D restrained case.

5.4   Numerical example

It is interesting to explore the consequence of the different boundary conditions on the unit volume volumetric expansion for the same crystal given saturation S_c and crystallisation pressure p_c. The matrix and crystal are supposed to have the same properties as the one used in the previous section:

$$k_m = 5.5 \qquad g_m = 4.1 \qquad b_m = 0.65 \qquad \varphi = 0.2 \qquad S_c = 0.3 \qquad k_c = 2k \qquad g_c = 2k \tag{29}$$

Using a Mori–Tanaka micro-mechanical scheme, these previous values furnish, in the case of a hydrostatic stress state, a value of the crystal Biot coefficient b_c^o of 0.113 and the following values for the macroscopic bulk and shear moduli: $K = 4.83$ GPa, $G = 3.63$ GPa.

The volumetric expansion obtained for a unit crystallisation pressure and for the different boundary conditions (restrained, unrestrained, etc.) is summarised in Table 1. For comparison, Table 2 contains the values obtained when neglecting the stress dependence of the crystal Biot coefficients. It is interesting to note that, the volumetric expansion is nearly two times smaller when the stress coupling effect on the Biot coefficients is taken into account. These results qualitatively explain the difference in the amount of expansion observed on cement with expanding additives in unrestrained and restrained conditions for different types of boundary conditions (Baumgarte et al., 1999).

Table 1   **Volumetric deformation, and stress components for the different types of boundary conditions ($p_c = 1$) when taking into account the non-linear stress dependence of the Biot coefficient. Compressive stresses are taken as positive**

	Unrestrained	1D Restrained	2D Restrained
ε^v	$2.3 10^{-5}$	$0.985 10^{-5}$	$0.617 10^{-5}$
σ_x	0	0	0
σ_y	0	0	0.1478
σ_z	0	1.45	0.1478
b_x	0.113	0.06	0.06
b_y	0.113	0.06	0.163
b_z	0.113	1.47	0.163

Table 2   **Volumetric deformation, and stress components for the different type of boundary condition ($p_c = 1$) when neglecting the non-linear stress dependence of the Biot coefficient. Compressive stresses are taken positive**

	Unrestrained	1D Restrained	2D Restrained
ε^v	$2.3 10^{-5}$	$1.86 10^{-5}$	$1.116 10^{-5}$
σ_x	0	0	0
σ_y	0	0	0.08
σ_z	0	0.067	0.08
b_x	0.113	0.113	0.113
b_y	0.113	0.113	0.113
b_z	0.113	0.113	0.113

6   Conclusions

Anisotropic far-field stresses modulate the orientation of growing crystals in porous media. The equilibrium configuration of a crystal is such that: i) the chemical activity of the pore solution is uniform around the crystal and ii) the stresses within the crystal are purely hydrostatic. In order to reach such an equilibrium under a far-field anisotropic stress state, the crystal orients its growth with respect to the far-field principal stresses direction and magnitudes. The consequence, at the macroscopic level of a representative volume element, is a non-linear stress dependent induced anisotropy of the poro-mechanical effect of in-pore crystallisation. Furthermore, this non-linear relationship of the macroscopic poro-mechanical parameters can be captured via a consistent micro-poro-mechanical up-scaling scheme. Preliminary computations on simple configuration and boundary conditions qualitatively reproduce experimental observations. Investigations of more complex boundary value problems and quantitative comparisons with experiments are underway.

Acknowledgements

References

Baumgarte, C., Thiercelin, M. and Klaus, D. (1999) Case Studies of Expanding Cement to prevent micro-annular Formation. In SPE Annual Technical Conference and Exhibition, number SPE 56535, Houston.

Berryman, J.G. (1997) Generalization of Eshelby's formular for a single ellipsoidal elastic inclusion to poroelasticity and thermoelasticity. Phys. Rev. Letters, 79(6), pp. 1141–1145.

Chatterji, S. (1995) Mechanism of expansion of concrete due to the presence of dead-burnt Ca0 and MgO. Cement Concrete Res., 25(1), pp. 51–56.

Coussy, O. (2005) Poro-mechanics of freezing materials. J. Mech. Phys. Solids, 53, pp. 1689–1718.

Coussy, O. (2006) Deformation and stress from in-pore drying-induced crystallisation of salt. J. Mech. Phys. Sol., 54, pp. 1517–1547.

Coussy, O. (2007) Revisiting the constitutive equations of unsaturated porous solids using a Lagrangian saturation concept. Int. J. Numer. Anal. Meth. Geomech., 31(15), pp. 1675–1694.

Coussy, O. and Monteiro, P. (2007) Unsaturated poroelasticity for crystallisation in pores. Computers and Geotechnics, 31, pp. 279–290.

Dewers, T. and Ortoleva, P.J. (1989) Mechano-chemical coupling in stressed rocks. Geochimica e Cosmochimica Acta, 53, pp. 1243–1258.

Durney, D.W. (1976) Pressure-solution and crystallisation deformation. Phil. Trans. R. Soc. Lond. A., 283, pp. 229–240.

Dvorak, G.J. and Benveniste, Y. (1992) On transformation strains and uniform fields in multiphase elastic media. Proc. R. Soc. Lond. A, 437, pp. 291–310.

Eshelby, J.D. (1957) The determination of the elastic field of an ellipsoidal inclusion and related problems. Proc. Roy. Soc., Series A, 241, pp. 376–396.

Flatt, R.J. (2002) Salt damage in porous materials: how high super-saturations are generated. J. Crystal Growth, 242, pp. 435–454.

Fuller, R.C., Prévost, J.H. and Piri, M. (2006) Three-phase equilibrium and partitioning calculations for CO2 sequestration in saline aquifers. J. Geophys. Res. B: Solid Earth, 111(6), pp. B06207.

Furuashi, R., Huang, J.H. and Mura, T. (1992) Sliding inclusions and inhomogeneities with frictional interface. J. Appl. Mech., 59, pp. 783–788.

Huang, J.H., Furuhashi, R. and Mura, T. (1993) Frictional Sliding Inclusions. J. Mech. Phys. Solids, 2(247–265), 41.

Huang, J.H. and Mura, T. (1992) Eshelby's tensor for an incoherent spherical inclusion. In ASME, (editor), Defects and anelasticity in the characterization of Crystalline Solids, pp. 61–70.

Kamb, W.B. (1959) Theory of preferred crystal orientation developed by crystallisation under stress. J. Geol., 67, pp. 153–170.

Kutchko, B., Strazisar, B., Dzombak, D., Lowry G. and Thaulow, N. (2007) Degradation of Well Cement by CO2 under Geologic Sequestration Conditions. Environ. Sci. Tech., 41, pp. 4787–4792.

Mura, T. (1982) Micromechanics of Defects in Solids. Martinus Nijhoff Publisher.

Mura, T. and Furuhashi, R. (1984) The elastic inclusion with a sliding interface. ASME J. Appl. Mech., 51, pp. 308–310.

Mura, T., Furuhashi, R. and Mori, T. (1987) Sliding Ellipsoidal in-homogeneities under shear. In G.C. Shih and S.E. Hsu (editors), Advanced Composite Materials and Structures, VNU Science Press, pp. 113–122.

Nemat–Nasser, S. and Hori, M. (1999) Micromechanics: Overall properties of heterogeneous materials. North-Holland, 2nd edition.

Paterson, M.S. (1973) Nonhydrostatic Thermodynamics and its Geological Applications. Rev. Geoph. Space Phys., 11(2), pp. 355–389.

Rijniers, L.A., Huinink, H.P. and Kopinga, K. (2005) Experimental Evidence of Crystallisation Pressure inside Porous Media. Phys. Rev. Lett., 94:075503–1–075503–4.

Ruedrich, J., Seidel, M., Rothert, E. and Siegesmund, S. (2007) Length changes of sandstones caused by salt crystallisation. Geol. Soc., London, Special Publications, 271, pp. 199–209.

Scherer, G.W. (1999) Crystallisation in pores. Cement Concrete Res., 29, pp. 1347–1358.

Zaoui, A. (2002) Continuum micromechanics: Survey. J. Engng Mech., 128(8), pp. 808–816.